

## Synthesis of Zinc Hydroxyfluoride Nanofibers through an Ionic Liquid Assisted Microwave Irradiation Method

Liyan Wu,<sup>[a]</sup> Jiabiao Lian,<sup>[a]</sup> Guixiang Sun,<sup>[a]</sup> Xiangrong Kong,<sup>[a]</sup> and Wenjun Zheng<sup>\*[a]</sup>

**Keywords:** Zinc / Fluorine / Microwave chemistry / Ionic liquids / Nanostructures

Zn(OH)F nanofibers were successfully synthesized from  $\text{Zn}_5(\text{OH})_8(\text{NO}_3)_2 \cdot 2\text{H}_2\text{O}$  by microwave irradiation in the presence of the ionic liquid [Tmim][BF<sub>4</sub>] (1,2,3-trimethylimidazolium tetrafluoroborate). The structure and morphology of the resulting Zn(OH)F nanofibers were investigated by XRD, SEM, and XPS, and the results indicate that the Zn(OH)F fibers are 80–200 nm in diameter and several micrometers

in length. A hydrogen bonding  $\pi$ – $\pi$  stacking mechanism is responsible for the 1D feature of Zn(OH)F. This method may be developed into a general way to synthesize other metal hydroxyfluoride nanostructures.

(© Wiley-VCH Verlag GmbH & Co. KGaA, 69451 Weinheim, Germany, 2009)

### Introduction

Zinc hydroxyfluoride is an important zinc-containing material. It has been demonstrated to be a catalyst for the formation of pyridine from tetrahydrofurfuryl alcohol and ammonia,<sup>[1]</sup> and it has been used as a precursor for ZnO.<sup>[2]</sup>

Zinc hydroxyfluoride is generally synthesized by hydrolysis–condensation of zinc fluoride tetrahydrate in water followed by evaporation at 100 °C to dryness. Zn(OH)F can be also obtained by thermal degradation of zinc fluoride (ZnF<sub>2</sub>) in air,<sup>[3]</sup> and more recently, it was observed on the surface of ZnO films after treatment with a NH<sub>4</sub>F aqueous solution.<sup>[4]</sup> However, the synthesis of nanostructured Zn(OH)F was rarely reported. Yu et al.<sup>[5]</sup> mentioned the synthesis of 1D nanostructured Zn(OH)F by the reaction between ZnO and NaF briefly in a communication, but no details were given. Recently, Huang et al.<sup>[1a]</sup> provided a hydrothermal route to synthesize net-like Zn(OH)F nanostructure at 120 °C.

Herein, we report a facile route to synthesize Zn(OH)F nanofibers from  $\text{Zn}_5(\text{OH})_8(\text{NO}_3)_2 \cdot 2\text{H}_2\text{O}$  in a water/[Tmim][BF<sub>4</sub>] (1,2,3-trimethylimidazolium tetrafluoroborate) system by microwave irradiation. The XRD pattern of  $\text{Zn}_5(\text{OH})_8(\text{NO}_3)_2 \cdot 2\text{H}_2\text{O}$  is shown in Figure S1 (Supporting Information). [Tmim][BF<sub>4</sub>] is a multifunctional reagent, as it can serve as both the source of the fluoride ions and the soft template. The synthetic method has the following obvious advantages: (1) The process is simple. (2) The products have high crystallinity and their morphologies can be

controlled by adjusting the concentration of [Tmim][BF<sub>4</sub>]. We believe that this method may be developed into a general procedure for the construction of metal hydroxyfluoride nanostructures.

### Results and Discussion

The X-ray powder diffraction (XRD) pattern in Figure 1a illustrates the phase characteristic of the Zn(OH)F nanofibers. The XRD pattern is readily indexed to orthorhombic Zn(OH)F (JCPDS file No. 74-1816). Minor ZnO peaks (marked by asterisks) were detected, and they are probably the result of the decomposition of  $\text{Zn}_5(\text{OH})_8(\text{NO}_3)_2 \cdot 2\text{H}_2\text{O}$  under the reaction conditions; pure Zn(OH)F can only be obtained by careful control of the stirring and heating process.

The elemental composition of the Zn(OH)F nanofibers was also appraised by X-ray photoelectron spectroscopy (XPS; Figure 1b). The presence of C, N, and B comes from the rudimental [Tmim][BF<sub>4</sub>] on the surface of the sample. The binding energies in the XPS spectrum were calibrated by using that of C 1s (284.6 eV). The binding energies of Zn 2p<sub>3/2</sub> and 2p<sub>1/2</sub> are identified to be 1022.2 and 1045.2 eV, respectively.<sup>[5,6]</sup> The binding energies of F 1s and O 1s are also identified to be 685.1 eV for F<sup>–</sup> and 533.3 eV for O<sup>2–</sup>.<sup>[5–7]</sup>

We monitored the phase and morphology evolution of the products synthesized at different concentrations of [Tmim][BF<sub>4</sub>] by XRD and SEM measurements. As shown in Figure S2a (Supporting Information), when the concentration of [Tmim][BF<sub>4</sub>] was varied from 0.0168 to 0.0336 M, Zn(OH)F was always obtained as the main phase. However, when the concentration of [Tmim][BF<sub>4</sub>] was equal to 0.0084 M, the phase of the product was close to the pure

[a] Department of Materials Chemistry, College of Chemistry, Nankai University, Tianjin 300071, P. R. China  
Fax: +86-022-23502458  
E-mail: zhwj@nankai.edu.cn

Supporting information for this article is available on the WWW under <http://dx.doi.org/10.1002/ejic.200900271>.

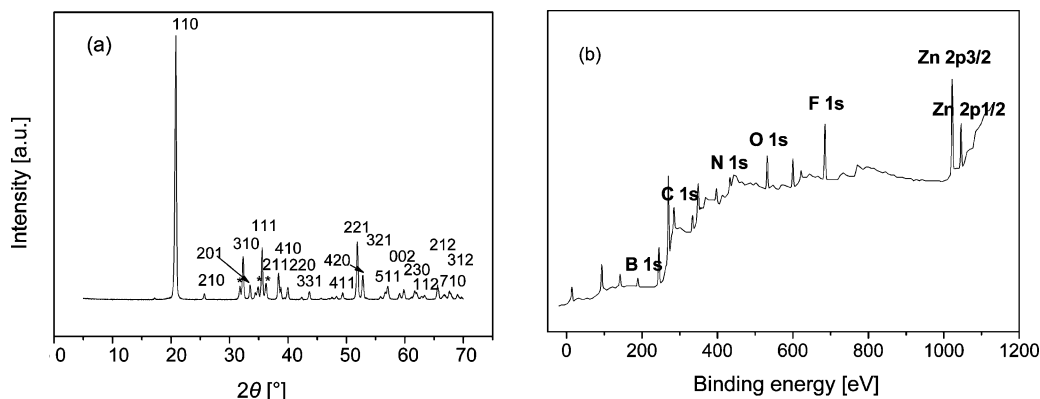


Figure 1. (a) XRD pattern and (b) XPS spectrum of Zn(OH)F nanofibers synthesized in the presence of 0.0253 M [Tmim][BF<sub>4</sub>]. Asterisk (\*) in (a) represents hexagonal ZnO (JCPDS file No. 80-0075).

hexagonal phase of ZnO (JCPDS file No. 80-0075), which has a submicron rod-like morphology (Figure 2a). When Zn(OH)F grows into the main phase, the fiber-like morphology becomes the dominant component in the SEM images. This result suggests that the high yield and well-defined nanofibers (Figure 2b–d) are Zn(OH)F. The diameters of the Zn(OH)F nanofibers are ca. 80–200 nm with a length up to several micrometers. Zn(OH)F was not stable toward electronic irradiation during recording of its HRTEM images. Thus, no HRTEM image is shown herein. Even though the amount of ZnO impurity can be decreased by increasing the concentration of [Tmim][BF<sub>4</sub>], the nanofibers are distinctly interwoven with some particles when the concentration of [Tmim][BF<sub>4</sub>] is equal to 0.0336 M. In contrast, a plethoric amount of ZnO impurity was obtained at a [Tmim][BF<sub>4</sub>] concentration of ca. 0.0168 M. The discussions above indicate that the [Tmim][BF<sub>4</sub>] concentration of ca. 0.0253 M may be suitable for the synthesis of Zn(OH)F nanofibers. In the literature reported by Biswick et al.,<sup>[8]</sup> the decomposition of  $\text{Zn}_5(\text{OH})_8(\text{NO}_3)_2 \cdot 2\text{H}_2\text{O}$  into  $\text{Zn}_3(\text{OH})_4(\text{NO}_3)_2$  and ZnO occurs at 120–140 °C, which may be responsible for the existence of the ZnO impurity in the present work.

Louër et al.<sup>[9]</sup> demonstrated the structure of  $\text{Zn}_5(\text{OH})_8(\text{NO}_3)_2 \cdot 2\text{H}_2\text{O}$ , which consists of infinite brucite-like layers, where one quarter of the octahedrally coordinated zinc atom sites are vacant and the zinc atoms are tetrahedrally coordinated by OH groups on either side of the empty/octahedra with a water molecule occupying the apex. Unbound nitrate groups are located between the sheets. According to the electronegative principle, the ability of  $\text{BF}_4^-$  to form hydrogen bonds is higher than that of  $\text{NO}_3^-$ . Consequently,  $\text{BF}_4^-$  will be allowed to substitute  $\text{NO}_3^-$ , and then it can intercalate into the interlayer gallery. Under the reaction conditions, the  $\text{BF}_4^-$  substituted precursor will decompose into Zn(OH)F, which means that the concentration of [Tmim][BF<sub>4</sub>] can be used to control the component of the final product. In the case of a [Tmim][BF<sub>4</sub>] concentration of 0.0084 M, no Zn(OH)F is observed after reaction because of the lower F<sup>−</sup> concentration.

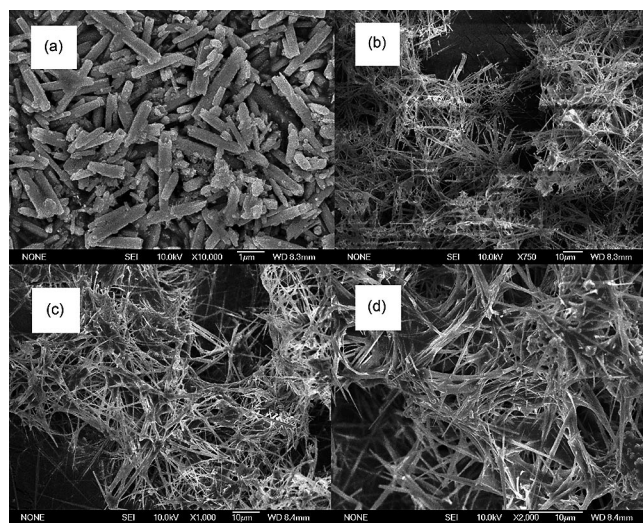


Figure 2. SEM images of the samples synthesized in different concentrations of [Tmim][BF<sub>4</sub>] with microwave irradiation for 60 min: (a) 0.0084 M; (b) 0.0168 M; (c) 0.0253 M; (d) 0.0336 M.

We also monitored the evolution of the morphologies of the samples at different reaction times by SEM. As shown in Figure S3 (Supporting Information), the  $\text{Zn}_5(\text{OH})_8(\text{NO}_3)_2 \cdot 2\text{H}_2\text{O}$  precursor has an irregular plate-like shape with a thickness of ca. 100 nm and a width of several microns, whereas a plentiful amount of rods and particles with smaller sizes are observed in the intermediate process. These suggest that the fracture of the precursor and the recrystallization of Zn(OH)F may be indispensable to the construction of the Zn(OH)F nanofibers.

In the structure of Zn(OH)F detailed by Serier et al.,<sup>[3]</sup> one of the two anionic sites is located at the intersection between two edge-sharing octahedra linked to a third octahedron by a corner and the other site is placed at the boundary of the three edge-sharing octahedra. In this structure, the (110) plane and its equivalent planes are highly populated by unique atoms in the low miller indices planes.

According to the crystallographic principle, these planes are thermodynamically stable planes of Zn(OH)F. This anisotropy may explain the 1D growth habit, which corresponds to the preponderant growth in the [001] direction. The quantitative crystallinity was estimated on the basis of the relative intensity of the (110) diffraction of Zn(OH)F (Figure S2b, Supporting Information). The change in the relative intensity through the concentrations of [Tmim][BF<sub>4</sub>] shows a  $\lambda$ -form curve, and a maximum value appears at a [Tmim][BF<sub>4</sub>] concentration of ca. 0.0253 M. This suggests that the ascendant growth in the [001] direction is responsible for the 1D feature of Zn(OH)F.

We<sup>[10]</sup> and others<sup>[11]</sup> have demonstrated the synthesis of nanostructures by an ionic liquid assisted route, and a hydrogen bonding  $\pi$ - $\pi$  stacking mechanism is helpful to understand the influence and control that the ionic liquids have on the morphologies of the nanostructures. In the present work, [Tmim][BF<sub>4</sub>] not only acts as a fluoride ion source, but it also can play a strategic role on the shape of Zn(OH)F as a soft template and capping agent. The formation of the Zn(OH)F nanofibers may be possibly explained by a hydrogen bonding  $\pi$ - $\pi$  stacking mechanism. As shown in Scheme 1b, the F-F distance in the BF<sub>4</sub><sup>-</sup> anion is about 2.28 Å,<sup>[12]</sup> which is close to the distance (ca. 2.1 Å)<sup>[3]</sup> between coplanar anions placed at each Zn(OH)<sub>3</sub>F<sub>3</sub> octahedron. Therefore, the (110) plane of Zn(OH)F is suitable to form a coverage layer through a BF<sub>4</sub><sup>-</sup> adsorbing model. Along with the BF<sub>4</sub><sup>-</sup> anions, the [Tmim]<sup>+</sup> cations will be also aligned and arranged along the (110) plane, driven by the coulomb coupling force. Ionic liquids are believed to facilitate the proposed relocation of the molecules on the basis of their ability to self-assemble into ordered structures. As shown in Figure S4 (Supporting Information), when NaF and NaBF<sub>4</sub> are used as fluoride ion sources, the relative intensity of the (110) diffraction is lower than that of the case when [Tmim][BF<sub>4</sub>] is used, whereas Zn(OH)F was observed as the main phase. It can be speculated that a hydrogen bonding  $\pi$ - $\pi$  stacking mechanism can rationally explain the influence of [Tmim][BF<sub>4</sub>] on the growth habit. As mentioned above, the change in the relative intensity through the concentrations of [Tmim][BF<sub>4</sub>] shows a  $\lambda$ -form

curve. We think this may be due to the viscosity of the medium. Other groups<sup>[13]</sup> have demonstrated that the viscosity of ionic liquid/water mixtures can generally be described by the exponential expression described in Equation (1):

$$\eta = \eta_{IL} \exp[-x_C/a] \quad (1)$$

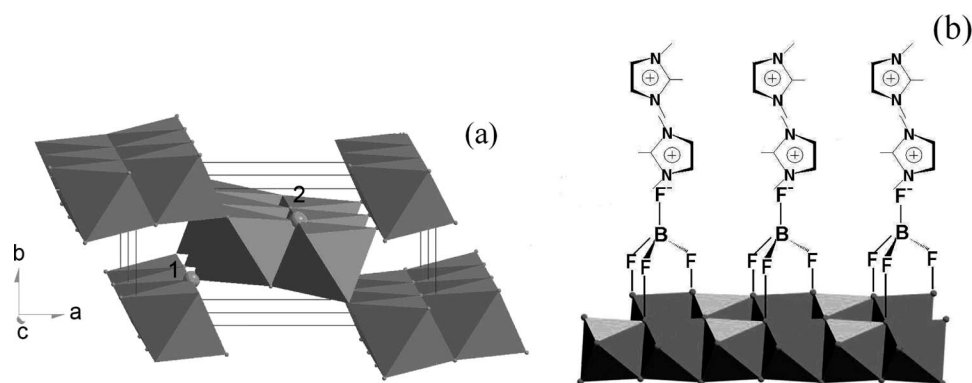
where  $x_C$  is the mole fraction of water,  $a$  is a characteristic constant of the mixture, and  $\eta_{IL}$  is the viscosity of the pure ionic liquid. The empirical equation [Equation (1)] indicated that the viscosity of the ionic liquid/water mixtures decreased exponentially when the mole fraction of water ( $x_C$ ) increased. In addition, water gradually volatilized from the reaction system with increasing the reaction time; the influence of viscosity on the Ostwald ripening of Zn(OH)F may be significant thereby. The exorbitant viscosity of the medium will restrict the diffusion velocity of the reactants; Ostwald ripening is, therefore, restrained to some extent. Consequently, the 1D feature and crystallinity of Zn(OH)F are not promoted but rather become worse when the concentration of [Tmim][BF<sub>4</sub>] is over 0.0253 M.

## Conclusions

In summary, well-defined Zn(OH)F nanofibers were successfully synthesized from Zn<sub>5</sub>(OH)<sub>8</sub>(NO<sub>3</sub>)<sub>2</sub>·2H<sub>2</sub>O in water/[Tmim][BF<sub>4</sub>] by microwave irradiation. The phase and morphology of the products can be controlled to some extent by adjusting the concentration of [Tmim][BF<sub>4</sub>]. A hydrogen bonding  $\pi$ - $\pi$  stacking mechanism is believed to be responsible for the self-assembly of [Tmim]BF<sub>4</sub> in the synthetic system, resulting in the formation of Zn(OH)F nanofibers. This method may be developed to serve as a potential way to fabricate other metal hydroxyfluoride nanostructures; moreover, the Zn(OH)F nanofibers as precursors could be used to construct ZnO nanofibers with hierarchical structures based on the decomposition process of Zn(OH)F.

## Experimental Section

Brucite-type Zn<sub>5</sub>(OH)<sub>8</sub>(NO<sub>3</sub>)<sub>2</sub>·2H<sub>2</sub>O was prepared by a reported route<sup>[14]</sup> and used as the precursor to fabricate Zn(OH)F nano-



Scheme 1. (a) Representation of the Zn(OH)F unit cell, in which all atomic positions correspond to a general 4a position [the structure provides only one 4a cationic site and two 4a anionic sites; sites 1 and 2 (bigger spheres) correspond to the presence of hydroxy or fluoride ions, respectively]; (b) schematic illustration of the proposed hydrogen bonding  $\pi$ - $\pi$  stacking mechanism.

fibers. In a typical procedure, the precursor (10 mmol) was suspended in water (50 mL) with different [Tmim][BF<sub>4</sub>] concentrations. The suspensions were heated by microwave irradiation for several minutes. The products were washed repeatedly with water and ethanol and then dried in an oven at 60 °C in air.

X-ray powder diffraction (XRD) measurements were performed with a Rigaku D/max-2500 diffractometer with Cu-K<sub>α</sub> radiation ( $\lambda$  = 0.154056 nm) at 40 kV and 100 mA. Scanning electron microscopy (SEM) was performed with a JSM 6700F field-emission scanning electron microscope. X-ray photoelectron spectroscopy (XPS) was performed with an ESCALAB II X-ray photoelectron spectrometer by using Mg-K X-ray as the excitation source.

**Supporting Information** (see footnote on the first page of this article): XRD pattern and SEM image of Zn<sub>5</sub>(OH)<sub>8</sub>(NO<sub>3</sub>)<sub>2</sub>·2H<sub>2</sub>O; XRD patterns of the products synthesized at different concentrations of [Tmim][BF<sub>4</sub>]; evolution of the relative intensity of the (110) reflection of Zn(OH)F synthesized at different concentrations of [Tmim][BF<sub>4</sub>].

## Acknowledgments

This work was supported by the National Natural Science Foundation of China (Grant No. 20571044) and the Project Fundamental and Applied Research of Tianjin (Grant No. 08JCYBJC00200).

- [1] a) Q. L. Huang, M. Wang, H. X. Zhong, X. T. Chen, Z. L. Xue, X. Z. You, *Cryst. Growth Des.* **2008**, *8*, 1412–1417; b) U. D. Nazirova, K. M. Akhmerov, P. Tashk, *Dokl. Akad. Nauk USSR* **1988**, *2*, 40–42.  
[2] N. Saito, H. Haneda, W. S. Seon, K. Koumoto, *Langmuir* **2001**, *17*, 1461–1469.

- [3] H. Serier, M. Gaudon, A. Demourgues, A. Tressaud, *J. Solid State Chem.* **2007**, *180*, 3485–3492.  
[4] S. Yamabi, H. Imai, *Trans. Mater. Res. Soc. Jpn.* **2003**, *28*, 329–331.  
[5] J. G. Yu, J. C. Yu, W. K. Ho, L. Wu, X. C. Wang, *J. Am. Chem. Soc.* **2004**, *126*, 3422–3423.  
[6] X. M. Hou, F. Zhou, F. W. M. Liu, *Mater. Lett.* **2006**, *60*, 3786–3788.  
[7] D. G. Huang, S. J. Liao, J. M. Liu, Z. Dang, L. Petrik, *J. Photochem. Photobiol. A: Chem.* **2006**, *184*, 282–288.  
[8] T. Biswick, W. Jones, A. Pacula, E. Serwicka, J. Podobinski, *J. Solid State Chem.* **2007**, *180*, 1171–1179.  
[9] M. Louër, D. Louër, D. Grandjean, *Acta Crystallogr., Sect. B* **1973**, *29*, 1696–1703.  
[10] W. J. Zheng, X. D. Liu, Z. Y. Yan, L. J. Zhu, *ACS Nano* **2009**, *3*, 115–122.  
[11] a) Y. J. Zhou, M. Antonietti, *J. Am. Chem. Soc.* **2003**, *125*, 14960–14961; b) A. Taubert, *Angew. Chem. Int. Ed.* **2004**, *43*, 5380–5382; c) T. Nakashima, N. Kimizuka, *J. Am. Chem. Soc.* **2003**, *125*, 6386–6387; d) H. Kaper, F. Endres, I. Djerdj, M. Antonietti, B. M. Smarsly, J. Maier, Y. S. Hu, *Small* **2007**, *3*, 1753–1763; e) J. M. Zhu, Y. H. Shen, A. J. Xie, L. G. Qiu, Q. Zhang, S. Y. Zhang, *J. Phys. Chem. C* **2007**, *111*, 7629–7633; f) Y. Zhou, J. H. Schattka, M. Antonietti, *Nano Lett.* **2004**, *4*, 477–481; g) Z. H. Li, Y. X. Luan, T. C. Mu, G. W. Chen, *Chem. Commun.* **2009**, 1258–1260; h) D. S. Jacob, L. Bitton, J. Grinblat, I. Felner, Y. Koltypin, A. Gedanken, *Chem. Mater.* **2006**, *18*, 3162–3168; i) L. X. Yang, Y. J. Zhu, W. W. Wang, H. Tong, M. L. Ruan, *J. Phys. Chem. B* **2006**, *110*, 6609–6614.  
[12] M. J. R. Clark, H. Lynton, *Can. J. Chem.* **1969**, *47*, 2579–2586.  
[13] a) J. J. Wang, Y. Tian, Y. Zhao, K. L. Zhuo, *Green Chem.* **2003**, *5*, 618–622; b) H. Xu, D. C. Zhao, P. Xu, F. Liu, G. Gao, *J. Chem. Eng. Data* **2005**, *50*, 133–135; c) C. Comminges, R. Barhdadi, M. Laurent, M. Troupel, *J. Chem. Eng. Data* **2006**, *51*, 680–685.  
[14] P. N. Steven, W. Jones, *J. Solid State Chem.* **1999**, *148*, 26–40.

Received: March 22, 2009

Published Online: June 5, 2009